Proc. Int. Symp. "Brittle Matrix Composites 6"
A.M. Brandt, V.C. Li, I.H. Marshall eds.
Warsaw, October 9-11, 2000
ZTUREK RSI and Woodhead Publ., Warsaw 2000

PLENARY INVITED PAPER

WHEN A CRACK IS NOT A CRACK

Victor C. Li
The ACE-MRL, Department of Civil and Environmental Engineering
University of Michigan, Ann Arbor, MI 48109-2125
USA

ABSTRACT

Brittle materials can be designed to be ductile composites by proper fiber reinforcement. A micromechanically designed Engineered Cementitious Composite (ECC) has demonstrated extreme damage tolerant behavior. In a number of studies of structural applications under monotonic or cyclic loads, ECC shows structural integrity even when damaged. This paper discusses the microcrack damage when the material undergoes pseudo strain-hardening in contrast to real cracks in tension-softening materials. The emphasis is on revealing that such microcrack damage, while seen as multiple cracks, are not cracks from the viewpoint of fracture mechanics and structural response.

Keywords
Crack, composites, ECC, strain-hardening, damage

INTRODUCTION

From a mechanical standpoint, a crack is often a precursor to structural failure by fracture. This is particularly so for brittle materials such as ceramics or concrete. In general, a crack may be regarded as a displacement discontinuity across which tensile traction is zero (a Griffith type crack) or decreasing with opening (tension-softening cohesive type crack). When a high enough tensile load is applied, such cracks invariably extends with increase in crack width. The condition for this to occur and the stability of extension are governed by well known linear and non-linear fracture mechanics.

Cracks are naturally of great concern to structural safety, and design of structures must take into account the presence and potential propagation of pre-existing cracks, and those that come about during service. In recent years, many attempts at improving the material and ductility of concrete structures by the use of fibers have been made (see, e.g. [1,2]). Most of these attempts have produced improved tension-softening materials, and material ductility generally refers to the more gradual descend of the softening branch of the tension-softening

curve when compared with the unreinforced material. However, these materials (including normal fiber reinforced concrete) remain susceptible to failure by localized fracture.

More recently, high performance fiber reinforced cementitious composites (HPFRCC) with macroscopic pseudo strain-hardening behavior have been developed [3]. Engineered Cementitious Composites (or ECC, for short) [4,5] is a special type of HPFRCC which are designed with optimized microstructures based on knowledge of micromechanics of fiber bridging [6] and steady state crack mechanics [7,8]. Deliberate choice of fiber, matrix and interface properties leads to minimized fiber content while the composite achieves strain capacity of as much as 7.5% [9] under uniaxial tensile load. During strain-hardening, multiple cracking occurs along the length of the specimen. The crack width often stabilizes and overall strain is accomodated by filling in of more multiple cracks until peak load is reached. These cracks are typically very fine, with width less than 200 μm even at peak load. In the macroscopic strain-hardening stage, the tensile traction across these fine cracks *increases* with crack width. Figure 1 shows the uniaxial tensile stress-strain curve of an ECC, together with the multiple microcrack damage pattern.

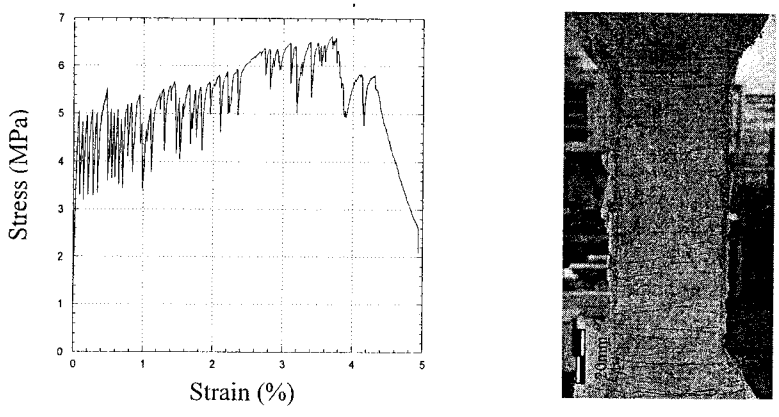

Figure 1. ECC tensile stress-strain behavior

In this article, it is emphasized that materials like ECC undergo an essentially damage process not unlike those in metals when overloaded. The dislocation plasticity in metal is replaced by microcrack inelasticity in ECC. Although such microcrack development appears to the eyes as cracks, they should be treated more as an inelastic damage behavior distributed over a volume of material. The process to localized fracture in a structural element is greatly delayed or totally eliminated. In this sense, these distributed microcracks are not the same as cracks normally known in concrete material.

In the following the damage behavior of ECC is contrasted with the real cracking behavior of concrete, using four experimental examples with different loading configurations. These include the tension-stiffening experiment, shear-beam experiment, column experiment, and beam-column joint experiment. The contrasting modes of failure are used to illustrate the theme of this article – when a crack is not a crack, in materials like ECC.

TENSION-STIFFENING EXPERIMENT

The tensile behavior of composite elements of steel reinforced ECC (R/ECC) and steel reinforced concrete (R/C) was studied by Li and Fischer [10]. Tensile load was applied to the single deformed steel reinforcing bar embedded inside a prism of matrix (concrete or ECC) with square cross-section. Prism dimension was 500 mm x 120 mm x 120 mm. Strain-gages were inserted into the reinforcing bar along the embedded length. A control gage was placed on the re-bar outside the matrix prism.

Figure 2a shows the familiar cracking behavior of the R/C specimen. Two large transverse cracks can be seen, together with some axial splitting and secondary cracks. Final failure occurs when the concrete completely detaches from the reinforcing bar. The maximum crack width at peak load is 6mm.

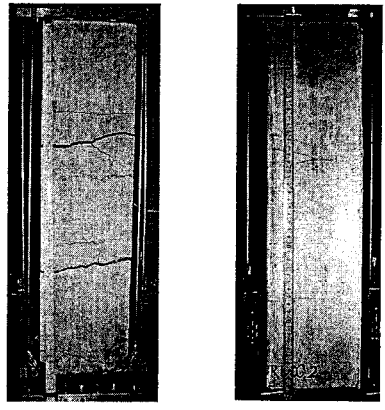

(a) (b)

Figure 2: (a) Fracture of Concrete in R/C Specimen, and (b) Damage Pattern in R/ECC Specimen

Figure 2b shows the fine multiple cracking behavior of the R/ECC specimen. About forty microcracks develop continuously along the specimen length up to peak load, with crack width remaining below 200μm. While the ECC matrix is damaged beyond 0.01% strain, no crack localization occurs up to about 4% overall strain of the specimen.

The strain gage readings at different applied load levels are plotted in Figure 3, for the case of R/C. At about 60 kN when the first concrete crack forms, strain jumps of a magnitude of 0.08% can be observed in the three gages (Gages at 150, 175 and 200 mm) located closest to the concrete crack. Subsequently the load-strain curve traces that of the control gage. These measurements clearly reveal the load shed by the concrete when it cracks, with the load picked up rapidly by the steel re-bar adjacent to the crack location. This phenomenon is well understood and the corresponding stress profiles in the concrete and in the steel can be illustrated as in Figure 4.

For the case of R/ECC, the strain gage readings (Figure 5) show a continuous increase with no sudden jumps during the multiple cracking process which started at about 0.01% overall strain. At each strain level, the applied load is higher for the composite (reflected by embedded gages) compared to the bare steel (reflected by the control gage). This stiffening effect continues even after steel yielding. Thus the multiple cracking process manifests itself as a "plastic" strain so that the deformation of the ECC remains compatible with that of the

steel re-bar. The stress profiles in the ECC and in the steel before and after formation of multiple cracks are illustrated in Figure 6.

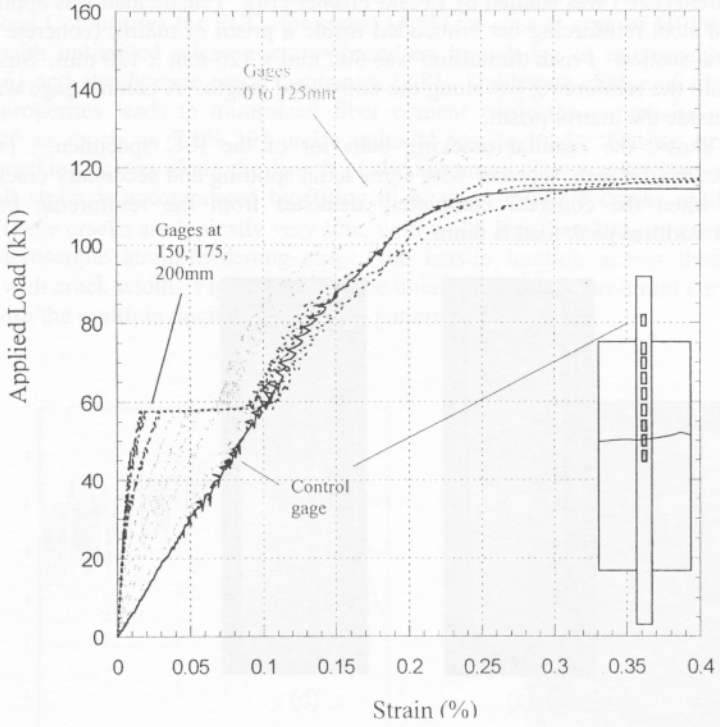

Figure 3. Strain-gage Readings as a Function of Applied Load Levels for R/C Specimen

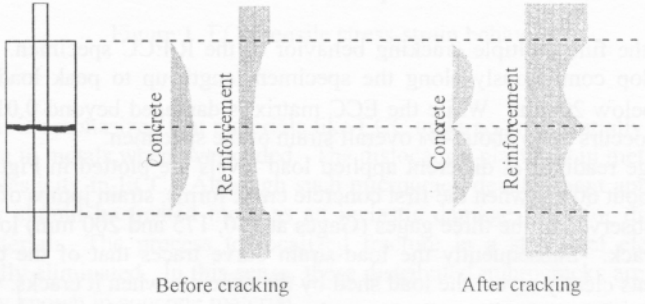

Figure 4. Schematic Stress Profiles in Steel and Concrete Before and After Cracking in R/C

Comparing between the cracking behavior in the R/C and in the R/ECC specimens, it should be clear that the crack in the concrete implies unloading of the matrix with subsequent stress and strain re-distributions. The high shear stress along the interface between the steel re-bar and the concrete at the crack site is responsible for the longitudinal crack and subsequent detachment of the rebar from the concrete. In contrast, the multiple cracks in the ECC

maintain load carrying capacity so that the ECC continues to share load with the re-bar, even at the microcracked sections. The compatible deformation can be expected to induce little or no shear stress along the interface, and no interface failure was observed. Final failure of the R/ECC specimen was due to plastic yielding and rupture of the steel bar outside the ECC prism.

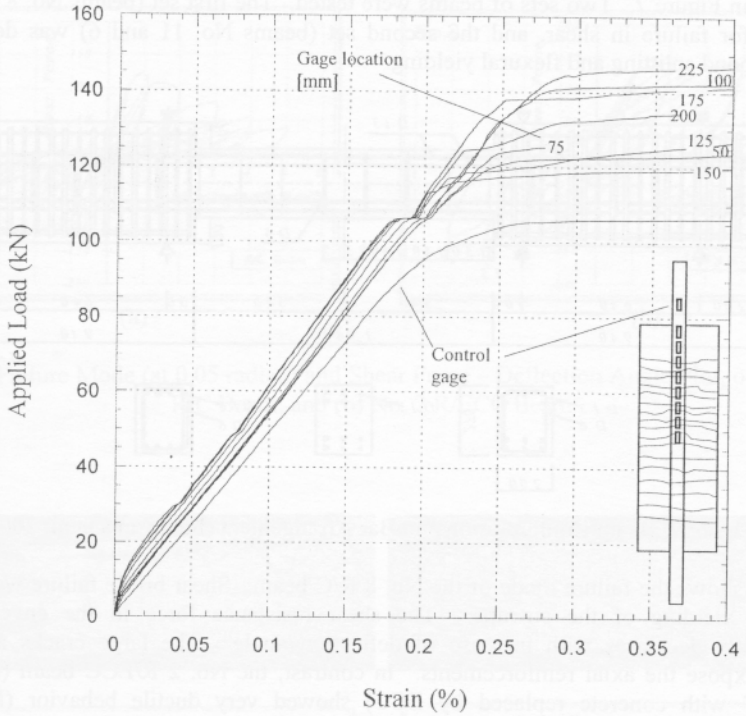

Figure 5. Strain-gage Readings as a Function of Applied Load Levels for R/ECC Specimen

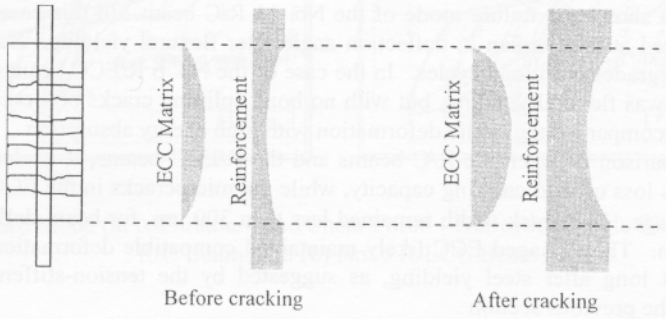

Figure 6. Schematic Stress Profiles in Steel and ECC Before and After Cracking in R/ECC

REINFORCED BEAM EXPERIMENTS

The shear resistance of reinforced concrete and ECC beams were studied by Kanda et al [11] and Fukuyama et al [12] under cyclic loading condition. Particular focus was placed on the beam performance upgrading effects of using ECC in place of concrete. The beam configuration and bar arrangements of the specimens used in the study of Fukuyama et al are as shown in Figure 7. Two sets of beams were tested. The first set (beams No. 8 and 2) was designed for failure in shear, and the second set (beams No. 11 and 6) was designed for failure in bond splitting and flexural yielding.

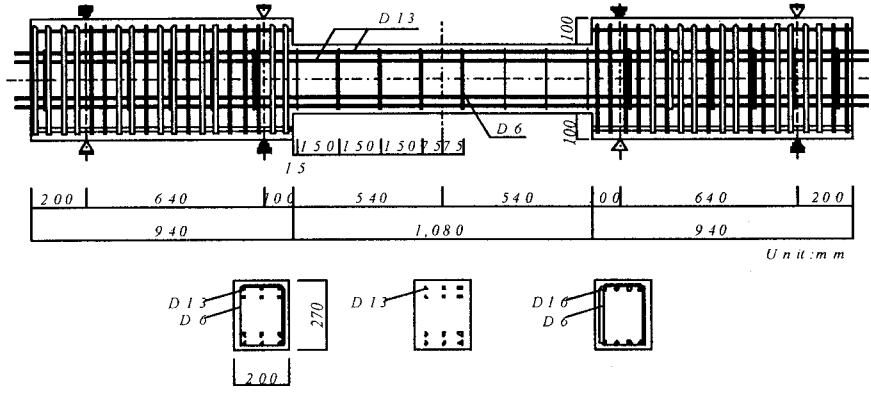

Figure 7: Beam Configuration and Bar Arrangement (Fukuyama et al, 2000)

Figure 8a shows the failure mode of the No. 8 R/C beam. Shear brittle failure was observed following yielding of the stirrups. The shear resistance force in the envelope curve subsequently decreases with increase of deflection angle. The large cracks and surface spalling expose the axial reinforcements. In contrast, the No. 2 R/ECC beam (identical to No.8 R/C with concrete replaced by ECC) showed very ductile behavior (Figure 8b). Yielding of the stirrups occurred much later in the load cycles, indicating that the ECC in its damaged mode with very fine cracks continued to function in resisting shear forces. Eventually flexural yielding was observed. The hysterisis loops show much higher energy absorption efficiency than that of the R/C beam.

Figure 9a shows the failure mode of the No. 11 R/C beam. In this case, bond splitting failure occurred at 0.02 radian in deflection angle after flexural yielding. Subsequently, the shear force degrades with load cycles. In the case of the No. 6 R/ECC beam (Figure 9b), the failure mode was flexural yielding, but with no bond splitting cracks observed. Instead very fine cracks accompanied the cyclic deformation with high energy absorption.

On comparison between the R/C beams and the R/ECC beams, it is clear that concrete cracks lead to loss of load carrying capacity, while the microcracks in the ECC are present as inelastic damage. The crack width remained less than 300 μm, for beam deflection angle up to 0.02 radian. The damaged ECC likely maintained compatible deformation with the steel reinforcement long after steel yielding, as suggested by the tension-stiffening experiment described in the previous section.

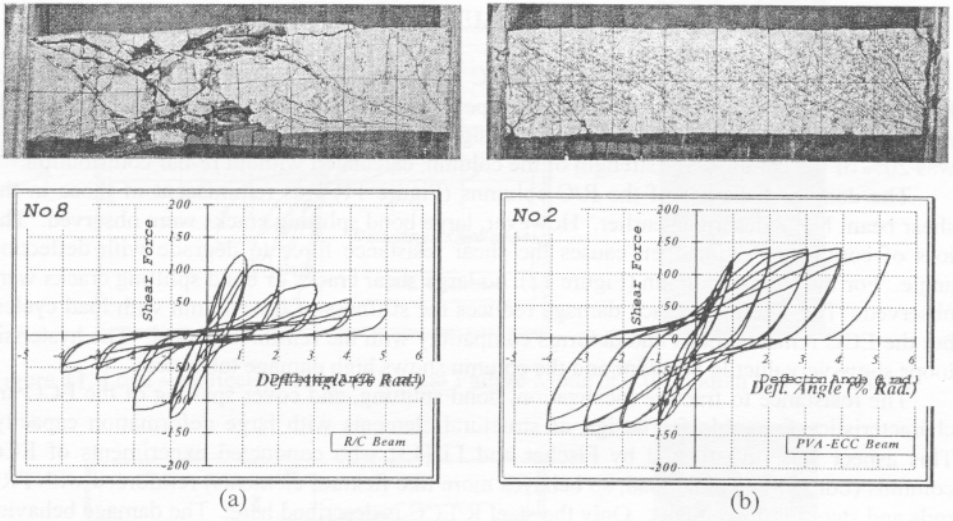

Figure 8. Failure Mode (at 0.05 radian) and Shear Force – Deflection Angle Plot, of (a) No.8 R/C Beam, and (b) No. 2 R/ECC Beam

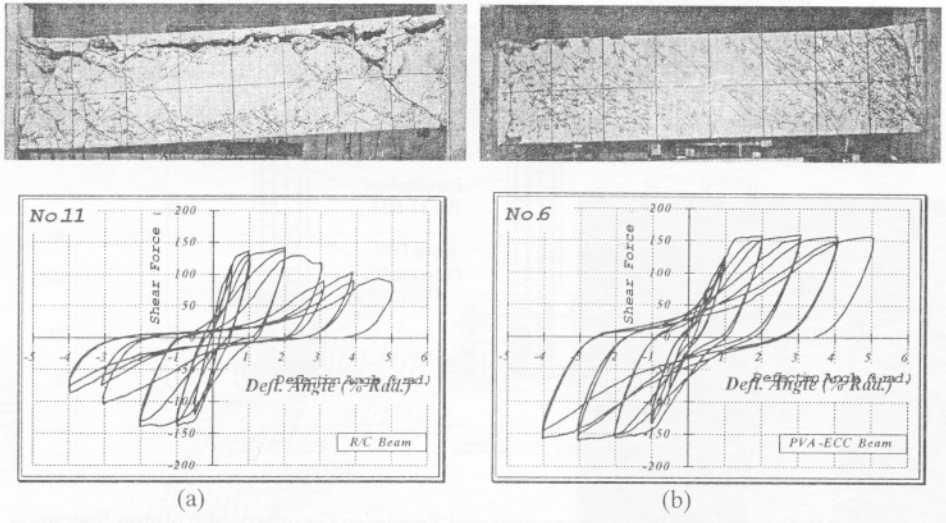

Figure 9. Failure Mode (at 0.05 radian) and Shear Force – Deflection Angle Plot, of (a) No.11 R/C Beam, and (b) No. 6 R/ECC Beam

REINFORCED COLUMN EXPERIMENTS

Column experiments with R/C and R/ECC were carried out by Fukuyama et al [12] under fully reversed cyclic loading condition. The specimen configuration and reinforcement details are shown in Figure 10. The column was designed to fail by shear. The axial force applied was 20% of the compressive strength of the column, calculated without re-bar contribution.

The damage behavior of the R/C columns (Figure 11) was reminiscent of those in the shear beam No. 8 described earlier. However, large bond splitting cracks were observed. The loss of composite action then causes the shear resistance force to degrade with deflection angle. For the R/ECC column (Figure 12), no large shear cracks or bond splitting cracks were observed. The fine microcrack damage reduces the stiffness of the column with load cycles, but the ECC remains intact and deforms compatibly with the reinforcing steel. The hysterisis loops show very ductile behavior and the column shows high damage tolerance.

The resistance to fracture localization, bond splitting, and cover spalling of the ECC are characteristics favorable for design of structural elements with large deformation capacity. This aspect was investigated by Fischer and Li [13] who conducted experiments of ECC columns (but with no axial load, so behaves more like flexural elements) reinforced with FRP rods and steel reinforcements. Only the steel R/ECC is described here. The damage behavior of the R/ECC element and its corresponding hysterisis loops are shown in Figure 13. The element shows very high ductility with the peak of the envelop reaching at 10% drift. The large energy absorption revealed by the full loops is due to the ability of the ECC to deform compatibly with the steel, so that steel yielding occurs over a long length instead of confined to the typical plastic hinge section of an R/C element.

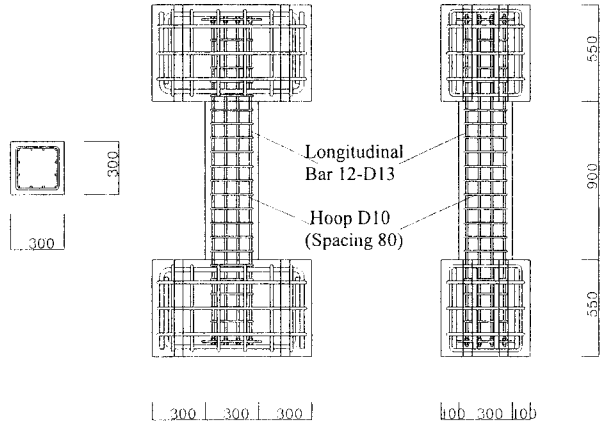

Figure 10. Reinforcing Bar Arrangement and Specimen Geometry of Column Specimen

From Figure 13a, it is clear that damage of the ECC in the form of microcracking (with crack width less than 200 μm) spreads over the length of the element. Below 5% drift, no localization of these cracks into fracture was observed. Final failure was due to rupture of the steel reinforcement at a drift of 15%.

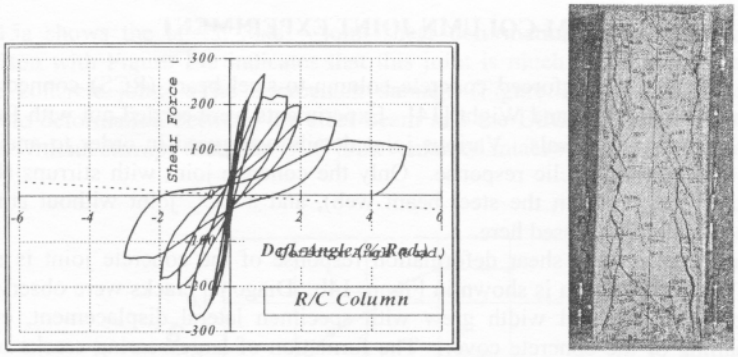

Figure 11. Load – Deflection Angle Plot and Failure Mode at 0.05 Radian of R/C Column

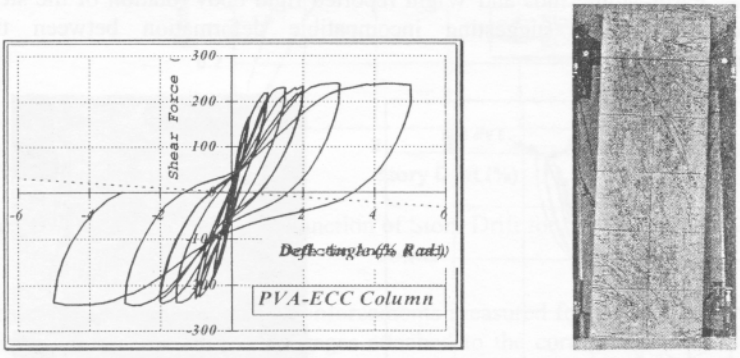

Figure 12. Load – Deflection Angle Plot and Damage Pattern at 0.05 Radian of R/ECC Column

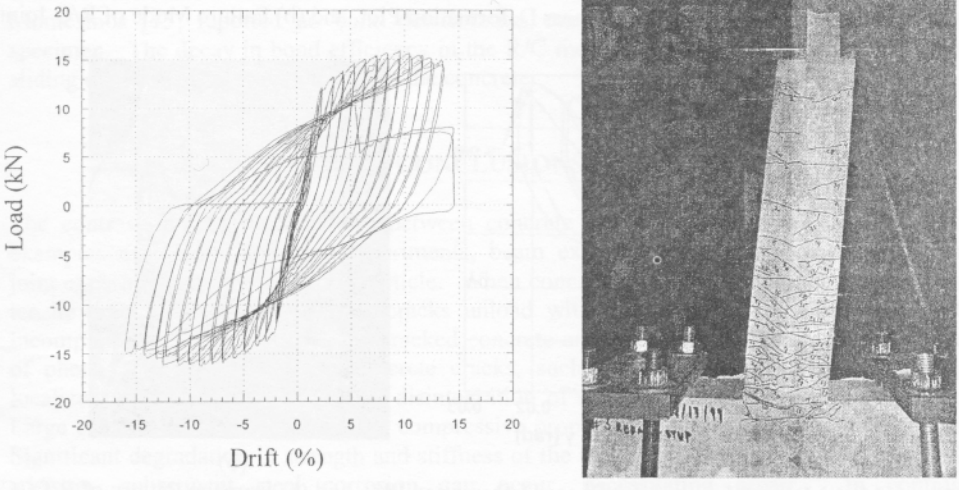

Figure 13. Load – Drift Plot and Damage Pattern at 10% Drift of R/ECC Element

BEAM-COLUMN JOINT EXPERIMENT

The seismic behavior of reinforced concrete column-to-steel beam (RCS) connections was studied by Parra-Montesinos and Wight [14]. Experiments were carried out with RCS joints subjected to large load reversals. Various joint details were used in order to analyze their influence on the inelastic cyclic response. Only the concrete joint with stirrups (U-shaped passing through drill holes in the steel beam web), and a ECC joint without stirrups but otherwise identical, are discussed here.

The lateral load – joint shear deformation response of the concrete joint is shown in Figure 14a. The crack pattern is shown in Figure 14b. Diagonal cracks were observed at 1% drift. The crack length and width grew with specimen lateral displacement, eventually leading to spalling of the concrete cover. The formation of large bearing cracks originated from the corners of the beam flanges is due to the stress concentration associated with the direct contact of the stiff tough steel with brittle concrete. Joint failure occurred at drift value of about 3.9%. Parra-Montesinos and Wight reported rigid body rotation of the steel beam inside the concrete joint, suggesting incompatible deformation between the two materials/elements.

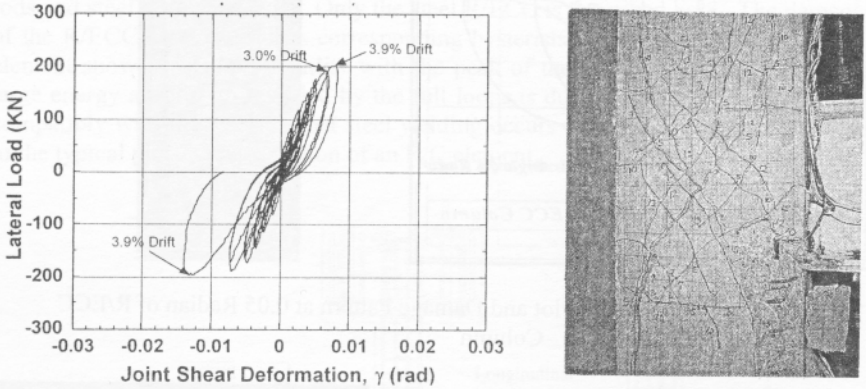

(a) (b)

Figure 14. (a) Lateral Load –Joint Shear Deformation Plot, and (b) Failure Mode of R/C Joint

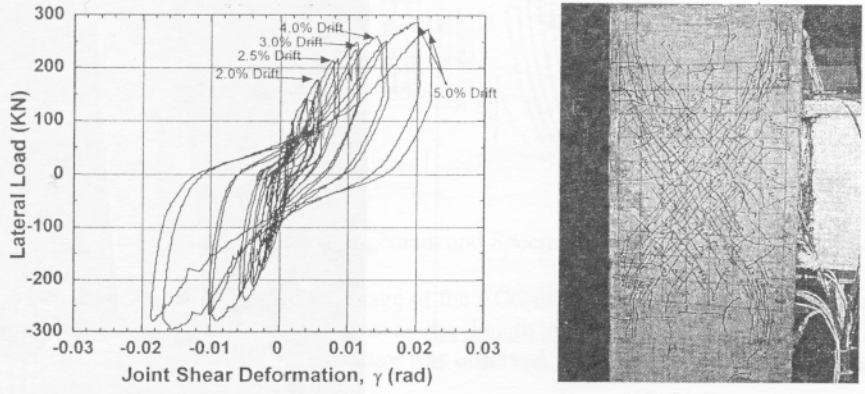

(a) (b)

Figure 15. (a) Lateral Load –Joint Shear Deformation Plot, and (b) Damage Pattern of R/ECC Joint

Figure 15a shows the lateral load – joint shear deformation response of the ECC joint. Comparison with Figure 14a indicates that this joint is much stiffer and stronger (by 50%) than the concrete joint. The microcrack damage (Figure 15b) did not compromise the compatible deformation between the steel beam and the ECC. Even after 20 cycles to 5% drift, and with no stirrups used, the ECC joint remained intact without requirement for repair.

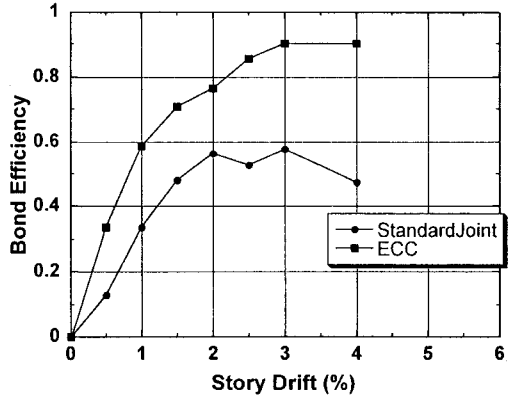

Figure 16. Bond Efficiency as a Function of Story Drift for the Standard R/C and R/ECC Joints

Bond efficiencies of column axial reinforcements measured for the two specimens (based on normalized strain differences from gages attached to the corner column bars over the joint depth) are shown in Figure 16. The bond efficiencies provide an indication between compatible deformation between the axial steel reinforcement and the surrounding concrete/ECC. High bond efficiency leads to more effective use of the axial reinforcement in maintaining stiffness and energy dissipation of the frame structure. It is clear that the R/ECC behaves much more coherently than the R/C connection, especially at large story drift. Parra-Montesinos [15] reported no bond deterioration even after steel yielding in the R/ECC specimen. The decay in bond efficiency in the R/C member beyond 2% story drift is due to sliding of the reinforcement relative to the concrete.

CONCLUSIONS

The contrast in inelastic behavior between concrete and ECC should be clear from the examples of tension-stiffening experiments, beam experiments, column experiments, and joint experiments described in this article. When concrete is loaded beyond its elastic range, tensile cracks are formed. These cracks unload with increasing crack width, leading to incompatible behavior between the cracked concrete and the steel reinforcement. A number of phenomena associated with concrete cracks, such as bond splitting, surface spalling, localized steel yielding, and general disintegration of the R/C element have been observed. Large cracks also lead to decrease in compressive properties in a direction parallel to cracks. Significant degradation in strength and stiffness of the reinforced element can then result. In addition, subsequent steel corrosion can occur, necessitating repair. In contrast, microcracking in ECC is akin to plastic yielding in metal. While ECC 'yields', tensile strain-

hardening maintains load carrying capacity. Such inelasticity associated with microcrack damage allows the ECC to maintain compatible deformation with the reinforcing steel. This damage tolerant behavior in turn provides excellent structural response, and minimize or eliminate the need for repair.

Although microcracking in ECC appears to the eyes as cracks, such cracks are very different from the cracks in brittle concrete. From a mechanical point of view, microcrack formation in ECC should be treated as inelastic damage, much like dislocation plasticity in metallic material. In this sense, just as plastic yielding in metallic materials are not treated as cracks, microcracking in ECC should also be distinguished from normal cracks in brittle concrete.

ACKNOWLEDGMENTS

The author acknowledges helpful discussions with Dr. Fukuyama at the Building Research Institute in Japan, and Dr. J. Wight at the University of Michigan, US. They also provided a number of figures (Figures 7-12 by Fukuyama and co-workers; Figures 14-16 by Wight and co-workers) for this article. Research in tension-stiffening and large deformation capacity element of R/ECC are part of a PhD study of G. Fischer, under the supervision of the author.

This work has been supported by grants from the US National Science Foundation (CMS-EQ-9601262; CMS-9872357).

REFERENCES

1. Balaguru, P., and Shah, S.P. Fiber Reinforced Cement Composites, McGraw Hill, New York, 1992, pp 530.
2. Banthia, N., Bentur, A. and Mufti, A. Fiber Reinforced Concrete: Present and the Future, Canadian Society for Civil Engineering, Montreal, 1998, pp 213.
3. Reinhardt, H., and Naaman, A. (Eds.) Proc. of High Performance Fiber Reinforced Cement Composites 3 (HPFRCC 3), Chapman & Hull, 1999, pp 666.
4. Li, V.C., From micromechanics to structural engineering -- the design of cementitious composites for civil engineering applications, JSCE J. of Struc. Mechanics and Earthquake Engineering, 10, 2, 1993, pp 37-48.
5. Li, V.C., Engineered cementitious composites – tailored composites through micromechanical modeling. In "Fiber Reinforced Concrete: Present and the Future", N. Banthia, A. Bentur, A. and A. Mufti eds. Canadian Society for Civil Engineering, Montreal, 1998, pp 64-97.
6. Li, V.C. and Leung, C.K.Y. Steady state and multiple cracking of short random fiber composites, ASCE J. of Engineering Mechanics 118, 11, 1992, pp 2246-2264.
7. Marshall, D.B. and Cox, B.N. A J-integral method for calculating steady-state matrix cracking stresses in composites, Mechanics of Materials 7, 1988, pp 127-133.
8. Li, V.C. and Wu, H.C. Conditions for pseudo strain-hardening in fiber reinforced brittle matrix composites, J. Applied Mechanics Review, 45, 8, 1992, pp 390-398.
9. Li, V.C., Wu, H.C., and Chan, Y.W. Effect of plasma treatment of polyethylene fibers on interface and cementitious composite properties, J. of Amer. Ceramics Soc., 79, 3, 1996, pp 700-704.
10. Li, V.C. and Fischer, G. Interaction between steel reinforcement and engineered cementitious composites. In "Proc. of High Performance Fiber Reinforced Cement

Composites 3 (HPFRCC 3)", H. Reinhardt and A. Naaman, eds. Chapman & Hull, 1999, pp 361-370.
11. Kanda, T., Watanabe S. and Li, V. C. Application of pseudo strain hardening cementitious composites to shear resistant structural elements. In "Fracture Mechanics of Concrete Structures" Proceedings FRAMCOS-3, AEDIFICATIO Publishers, D-79104 Freiburg, Germany, 1998 pp 1477-1490.
12. Fukuyama, H., Matsuzaki, Y., Sato, Y. Iso, M. and Suwada H. Structural performance of engineered cementitious composite elements, to appear in the proceedings of the ASCCS-6-2000, 2000.
13. Fischer, G. and Li, V.C. Structural composites with ECC, to appear in the Proceedings of the ASCCS-2000, 2000.
14. Parra-Montesinos, G.J., and Wight J.K. Behavior and strength of RC column-to-steel beam connections subjected to seismic loading, to appear in the Proceedings of the 12th WCEE, 2000.
15. Parra-Montesinos, G.J., Seismic Behavior, Strength and Retrofit of Exterior RC Column-to-Steel Beam Connections, PhD Thesis, University of Michigan, Ann Arbor, 2000.